Available online at www.sciencedirect.com
SciVerse ScienceDirect
Ceramics International 38 (2012) 5835–5842
CERAMICS INTERNATIONAL
www.elsevier.com/locate/ceramint

Logotype-selective electrochromic glass display

Chien Chon Chen [a], Wern Dare Jheng [b,*]

[a] Department of Energy Engineering, National United University, Miaoli 36003, Taiwan
[b] Department of Mechanical Engineering, National Chin-Yi University of Technology, Taichung 411, Taiwan

Received 24 September 2011; received in revised form 5 April 2012; accepted 11 April 2012
Available online 24 April 2012

Abstract

This paper describes a fabrication method of a logotype-selective electrochromic (EC) glass. The EC glass performance based on the sample size, WO_3 film thickness, and internal impedances under various applied voltages are also discussed. The logotype-selective electrochromic glass was fabricated by the sputter deposition process. Both working and counter electrode were coated with ITO/WO_3 films. The specific logotypes of ''NCUT'' and ''NUU'' can be displayed with positive and negative voltages applied to the EC glass. EC glasses of various sizes (1 cm^2, 4 cm^2, 9 cm^2, 25 cm^2, and 100 cm^2) were also fabricated by sputter deposition process. When voltage (-3.5 V) was applied to the device, the active layer of the assembled device changed from almost transparent to a translucent blue color (colored). The average transmittance in the visible region of the spectrum for a 100 cm^2 EC device was 73% in the bleached state. The best device, with a 140 nm WO_3 active layer, had average transmittances in the colored and bleached states of 11.9% and 54.8%, respectively. Cyclic voltammogram tests showed that reproducibility of the colored/bleached cycles was good. Nyquist plots showed that increasing the device size decreased the current density, and the electrolyte impedance increased because of a low conductive electrolyte in the device.

Keywords: Impedances; Electrochromic glass; Sputter deposition; Blue color; Bleached

1. Introduction

Electrochromic (EC) devices are of interest in different fields of technology. Among the numerous possible applications, one is the information display. Tungsten oxide is by far the most extensively studied EC material. Highly disordered WO_3 films are usually employed in work on EC. In general, an EC window consists of four layers. Two layers of conducting oxide material, adjacent to the glass layers, supply the voltage to the central two layers, consisting of an ion conducting/electrolyte layer and an EC layer (typically WO_3). All the layers are normally transparent to visible light. In recent years, there have been sustained efforts to develop EC technology and devices. Many companies are continuously working to complete the commercialization process. To implement this technology, their products must be capable of coloring and bleaching thousands of times with little or no performance loss. EC windows enable the changing of their optical transmittance by applying appropriate electrical signals to the window structure. In many applications, such as ''smart'' EC buildings where windows are required, control of the window's transmittance is automated to ensure a constant level of transmitted daylight for different outdoor illuminations.

In recent years, the nanometer technological progress has led to the creation of many special new materials. Therefore now, information photoelectricity, catalysis, and magnetism have broader application domains because of nanotechnology. For example, the tungsten oxide (WO_3) semiconductor, which has rich special physics and chemical properties, is widely treated as electrochromic (EC) [1], photochromic [2,3], gasochromic [4], catalyzed [5], and hide material [6], and it even has potential as a superconducting material [7]. Since the 1980s, to further develop its application domain using the WO_3 fine performance, many researchers have reduced the crystal grain size to increase the surface effect [8,9]. The manufacturing methods include sol–gel [10], sputter [11], evaporation [12,13], chemical vapor deposition [14], and anodization [15,16].

One group of chromogenic optically switching materials displays reversible spectral coloration–bleaching when they are

* Corresponding author.
E-mail address: jen102@ncut.edu.tw (W.D. Jheng).

0272-8842/$36.00
http://dx.doi.org/10.1016/j.ceramint.2012.04.033

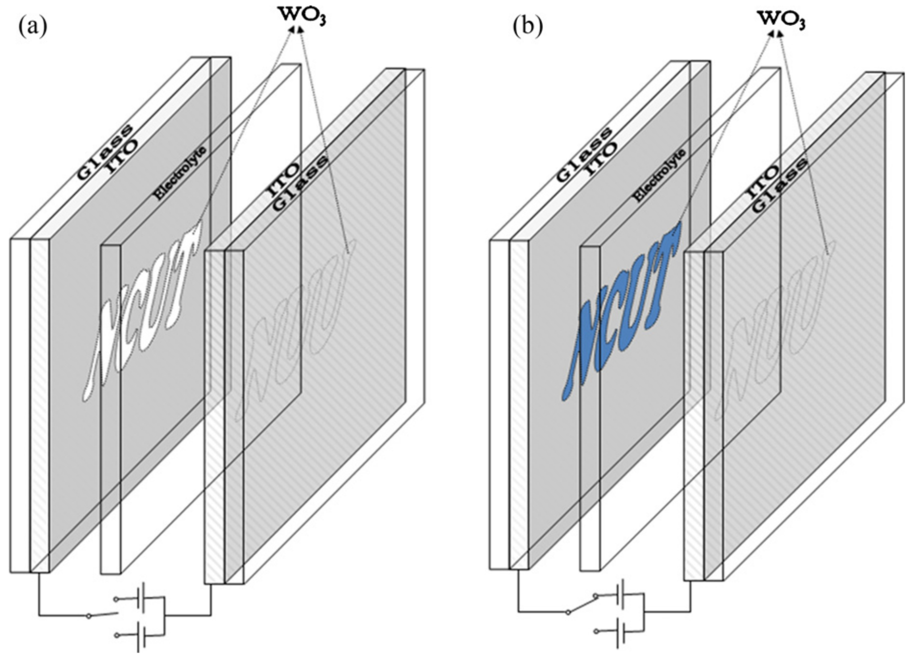

Fig. 1. Schematic diagram of the logotype-selective electrochromatic glass structure; (a) logotypes of ''NCUT'' and ''NUU'' of WO_3 films were coated on both ITO glass. (b) ''NCUT'' was observed in the negative voltage state.

subjected to double charges and monovalent cation injection–extraction. Valve metals such as Al, Ti, Sn, Nb, and W can form a thick oxide film of Al_2O_3 [17], TiO_2 [18], SnO_2 [19], Nb_2O_5 [20], and WO_3 [21] through anodization. Aggressive ions like chloride and fluoride are usually added to the electrolyte to attach to the compact barrier and form porous anodic film. Transition metal oxides of WO_3 have transparent and semiconducting physical characteristics, making them suitable for electrochromic (EC) devices [22–25]. In EC glass, the transmittance of WO_3 films can be altered in a reversible and persistent manner by the intercalation/de-intercalation of small cations (H^+, Li^+, Na^+) and electrons into the film.

To enhance the application of EC glass, we fabricated a logotype-selective electrochromic (EC) glass, which can alternate between logotypes of ''NCTU'' and ''NUU'' under alternating negative and positive voltages. We also fabricated EC glass samples of various sizes and evaluated the device performance by UV–VIS–NIR optical photometer, cyclic voltammetry (CV), and electrochemical impedance spectroscopy (EIS) tests.

2. Experimental

EC glass has a configuration of glass/ITO/WO_3/1 M $LiClO_4$-PC/ITO/glass. The WO_3 thin film was deposited onto ITO (10 Ω/sq) glass by RF magnetron sputtering using a 4-in. tungsten metal target with a purity of 99.99%. A mixture of argon and oxygen gasses with a ratio of Ar/O_2 of 3 was used for the deposition. The base pressure of the deposition chamber was kept at 1×10^{-6} Torr. Working pressure was set to 5×10^{-3} Torr, and sputtering power during deposition was 100 W for 10–120 min. The thickness of the WO_3 film ranged from about 10 to 140 nm. A sample of 10 cm × 10 cm EC glass

(a)

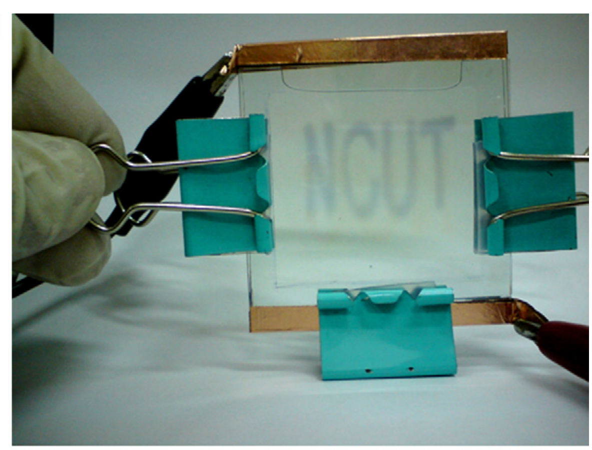

(b)

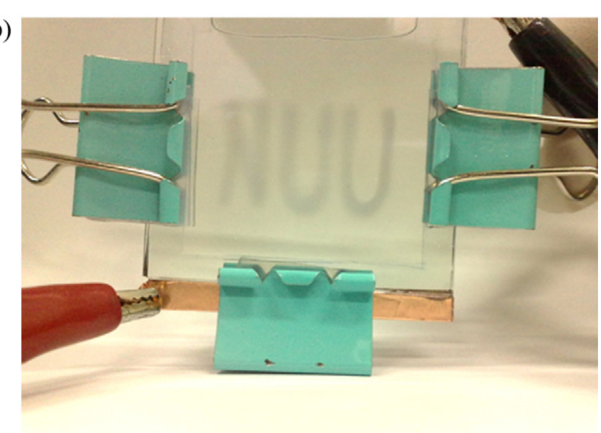

Fig. 2. Photograph of EC glass devices (a) in the negative voltage state (''NCUT''), and (b) in the positive voltage state (''NUU''), respectively.

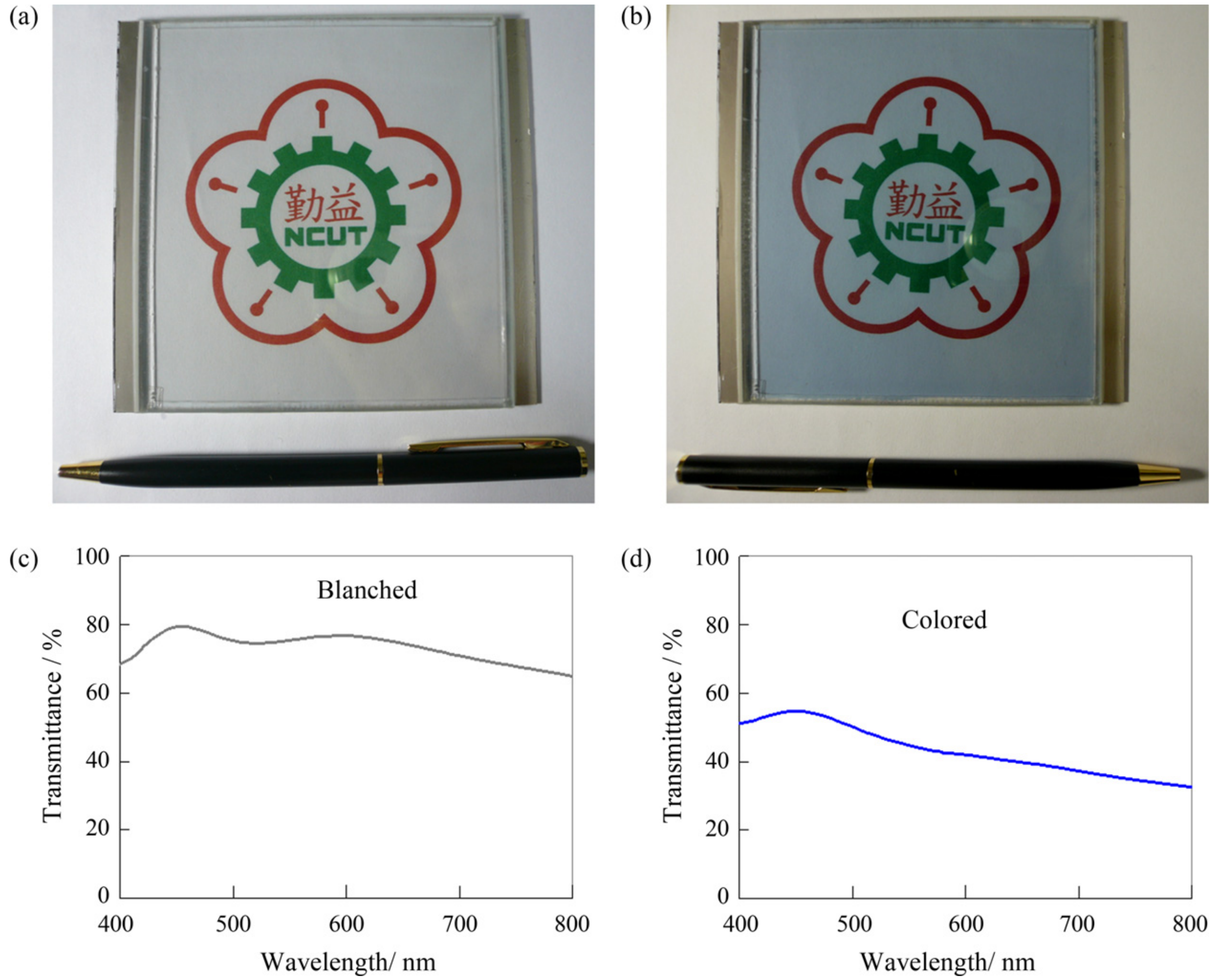

Fig. 3. Images of the electrochromatic glass devices and optical transmittance spectrum. (a) EC glass with transparent characterization in a bleached state, (b) EC glass with blue color translucent characterization in a dyed state, (c) the glass in the visible light range has 73% and (d) 55% transparency in the bleached and dyed states.

was obtained by assembling two pieces of the ITO glass in the following way. The two electrodes were assembled into a sandwich-type cell and sealed with hot-melt film (SX1170, Solaronix, thickness 0.1 mm), and electrolyte was injected into the space between the two electrodes with a syringe. The device was then sealed with vacuum glue. The optical transmission and reflection spectra were recorded using a UV–VIS–NIR optical photometer (JASCO V570) with an integrating sphere (JASCO ISN-470) in the range from 400 to 800 nm. The electrochromic properties were characterized using the cyclic voltammetry (CV) method by impedance Measuring Unit (IM 6) from Zahner. Two electrodes were used to perform the electro-chemical tests in an electrolyte of a 1 M $LiClO_4$ in propylene carbonate solution. The internal impedance was evaluated by the electrochemical impedance spectroscopy (EIS) results.

3. Results and discussion

Electrochromatic glass includes transparent substrates (glasses), working electrode (ITO/WO_3), ion conductive layer (1 M $LiClO_4$-PC), and counter electrode (ITO/WO_3). Both working and counter electrodes in this study were composed of the same ITO/WO_3 films, but WO_3 films with different logotypes were deposited on the electrodes. Fig. 1 shows a schematic diagram of a logotype-selective EC structure. First, logotypes of ‘‘NCUT’’ and ‘‘NUU’’ were made on the ITO glasses using the tape masking method. Then the unmasked areas of ‘‘NCUT’’ and ‘‘NUU’’ were deposited with WO_3 films, in which both electrodes served as working electrode or counter electrode (Fig. 1(a)). The result was marked areas of ITO films and unmarked areas of WO_3 deposition film. Whether positive or negative voltage was applied to the working electrode was controlled with a power switch. When the negative voltage was applied to the electrode with the NCUT logotype, which served as a working electrode, and the electrode with the NUU logotype, which served as a counter electrode, the EC glass presented the blue NCUT logotype (Fig. 1(b)). When the positive voltage was applied, the EC glass presented the blue NUU logotype. For example, Fig. 2 shows photographs of the EC glass device: (a) is the negative voltage state (‘‘NCUT’’), and (b) is the positive voltage state (‘‘NUU’’), respectively.

In order to investigate the blanched/colored property in a large size EC glass, we made a 10 cm × 10 cm EC glass. This

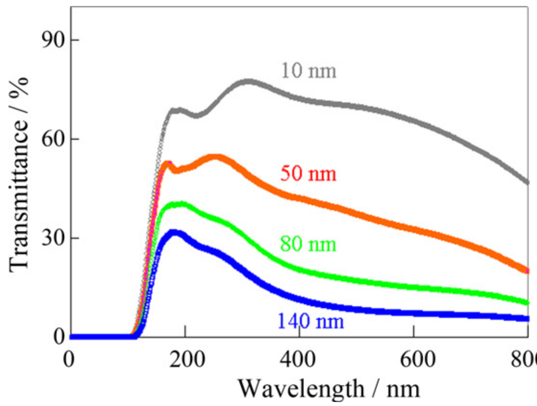

Fig. 4. Transmission spectra of EC glass with various WO_3 film thicknesses. The device with (a) 10 nm, (b) 50 nm, (c) 80 nm, and (d) 140 nm WO_3 film thickness has 60.7%, 34.8%, 19.6%, and 11.9% transparency, respectively, in the visible light range in the bleached state (−3.5 V).

large size EC glass has a typical structure of glass/ITO/WO_3 as a working electrode, 1 M $LiClO_4$-PC, as electrolyte, and ITO/glass as a counter electrode. Fig. 3 shows photographs of 10 cm × 10 cm EC glass devices and the optical transmittance spectrum. Fig. 3(a) is the as-prepared state and shows the transparent state (blanched). In Fig. 3(b), when voltage (−3.5 V) was applied to the device, the active layer of the assembled device changed from being almost transparent to a translucent blue color (colored). The device had 62.1% (Fig. 3(c) and (d)) 34.8% (Fig. 3(d)) transparency in the visible light range in the blanched and dyed states. In the colored process, electrons are injected into the EC layer (WO_3) from the ITO and cation (Li^+) from the electrolyte. The reverse happens for the bleaching process. The electron-transfer reaction occurs within the thin films of EC oxide (WO_3) sandwiched between a transparent electrode of ITO coated glass substrates and an electrolyte, allowing for ready conduction of the Li^+ ion needed for the charge balance in solid-solution electrodes. Fig. 4 shows the transmission spectra of EC glass with various WO_3 film thicknesses. When the device had an active layer, the WO_3 film thicknesses were (a) 10 nm, (b) 50 nm, (c) 80 nm, and (d) 140 nm, and the transmittances were 60.7%, 34.8%, 19.6%, and 11.9% transparency, respectively, in the visible light range in the bleached state (−3.5 V). The transmittance decreased as the film thickness increased. Fig. 5 shows the transmission spectra

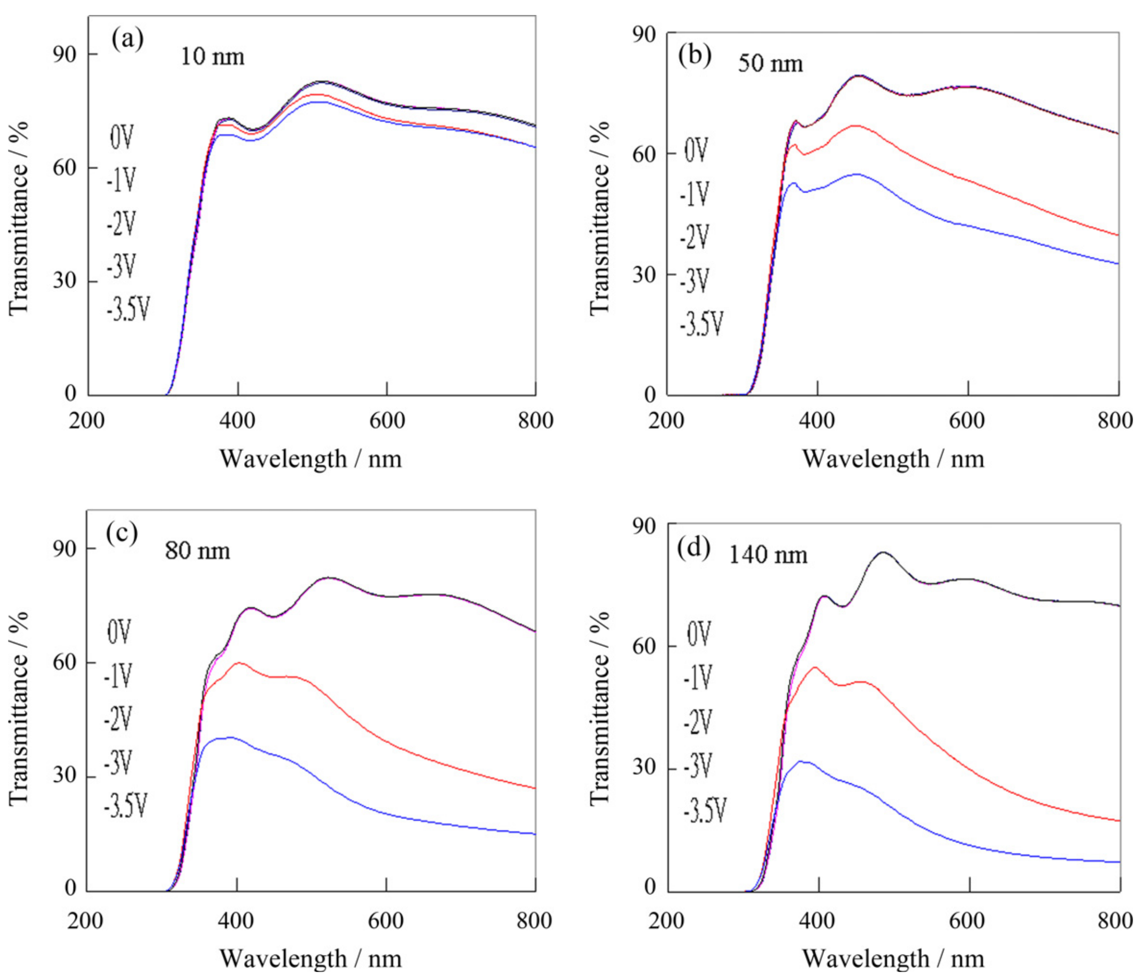

Fig. 5. Transmission spectra of EC glass with various WO_3 film thicknesses and applied voltages. When 0 V, −1 V, −2 V, −3 V, and −3.5 V was applied to the EG glass, the device with (a) 10 nm had transparencies of 65.5%, 64.2%, 63.6%, 61.6%, 60.7%, (b) 50 nm, 62.1%, 61.8%, 60.5%, 42.5%, and 34.8%; (c) 80 nm, 61.7%, 61.5%, 59.8%, 33.1%, and 19.6%; and (d) 140 nm, 61.0%, 60.6%, 59.7%, 25.3%, and 11.9%, respectively, in the visible light range in the bleached state.

Table 1
Transmission spectra of EC glass with 10 nm, 50 nm, 80 nm, and 140 nm WO_3 film thicknesses in the colored (0 to −3.5 V) and bleached (1–3.5 V) states. The device with 140 nm WO_3 film thicknesses had 61.0%, 11.9%, and 54.8% transmittance in the original, colored, and bleached states, respectively.

	Original	Colored				Blanched			
Applied voltage (V)	0	−1	−2	−3	−3.5	1	2	3	3.5
Transmittance %									
10 nm	65.5	64.2	63.6	61.3	60.7	61.1	64.3	65.1	65.2
50 nm	62.1	61.8	60.5	42.5	34.8	50.7	58.7	59.7	60.0
80 nm	61.7	61.5	59.8	33.1	19.6	28.9	50.3	54.8	56.5
140 nm	61.2	60.6	59.7	25.3	11.9	20.1	48.9	54.6	54.8

of EC glass with various WO_3 film thicknesses and applied voltages. The device with (a) 10 nm WO_3 film had average transparencies of 65.5%, 64.2%, 63.6%, 61.6%, and 60.7% transparency in the visible light range under 0 V, −1 V, −2 V, −3 V, and −3.5 V voltage applied in a bleached state; (b) 50 nm WO_3 film had average transparencies of 62.1%, 61.8%, 60.5%, 42.5%, and 34.8%; (c) 80 nm WO_3 film had average transparencies of 61.7%, 61.5%, 59.8%, 33.1%, 19.6%; and (d) 120 nm WO_3 film had average transparencies of 61.0%, 60.6%, 59.7%, 25.3%, and 11.9%. Details of the transmittance values are shown in Table 1. The results show that the differences in transmittance of 10 nm, 50 nm, 80 nm, and 120 nm active layers in the EC glass were 4.5%, 25.2%, 36.9%, and 42.9% between −3.5 V (colored) and 3.5 V (bleached). Also, the clear color change in the device was noted when the applied voltage was below −3 V (colored) and above 2 V (bleached).

Fig. 6 shows the results of cyclic voltammetry of EC glass performed between −3 V and +3 V with a scan rate of 100 mV in 1 M $HClO_4$-PC electrolyte. Because of the low conductive electrolyte in the device, the current density decreased with increases in sample size from (a) 1 cm^2 to (b) 4 cm^2, (c) 9 cm^2, and (d) 25 cm^2. The voltammograms clearly show all the samples had better reversibility and reproducibility in their electrochemical analysis. When the EC device was in the colored state (negative voltage) Li^+ ion was doped into WO_3 film. The quantity of Li^+ ions moving in and out of the WO_3

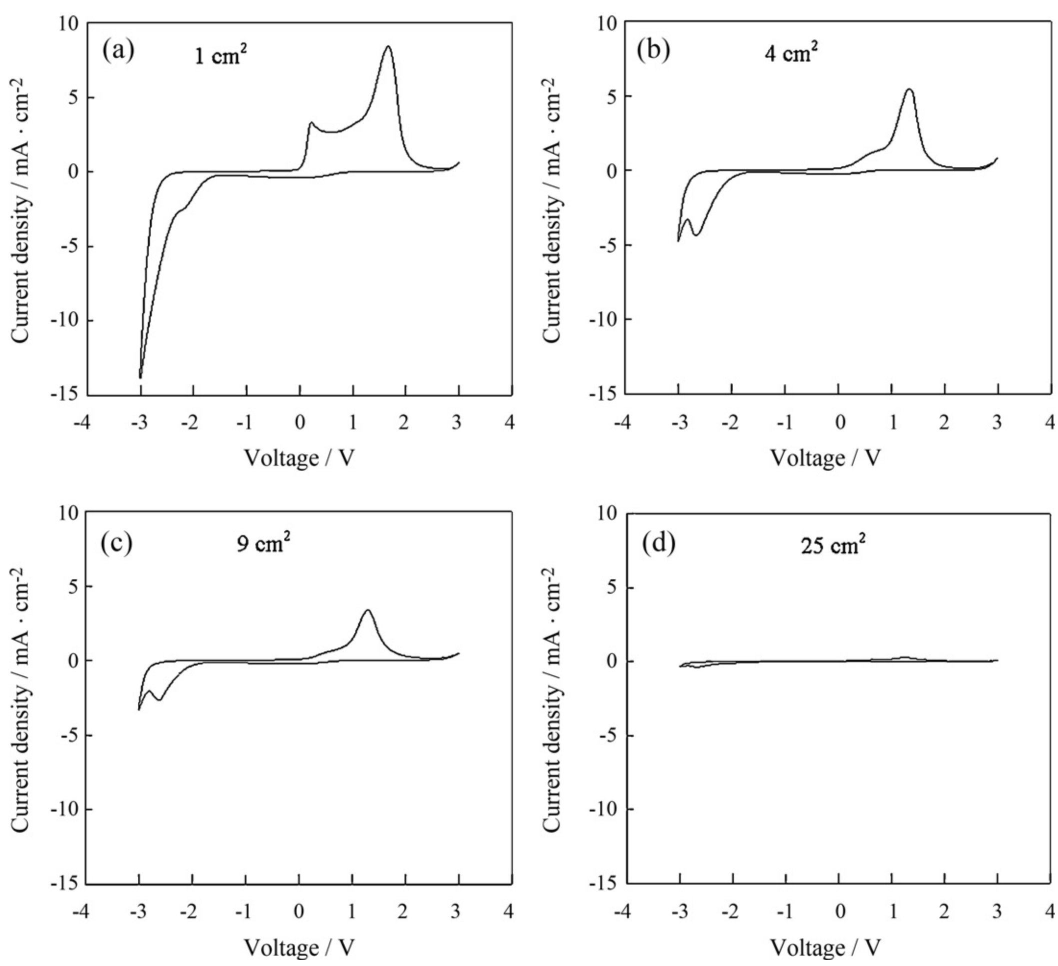

Fig. 6. Cyclic voltammetry of EC glass performed between −3 V and +3 V with a scan rate of 100 mV in 1 M $HClO_4$-PC electrolyte. The current density decreased with increases in sample size from (a) 1 cm^2 to (b) 4 cm^2, (c) 9 cm^2, and (d) 25 cm^2.

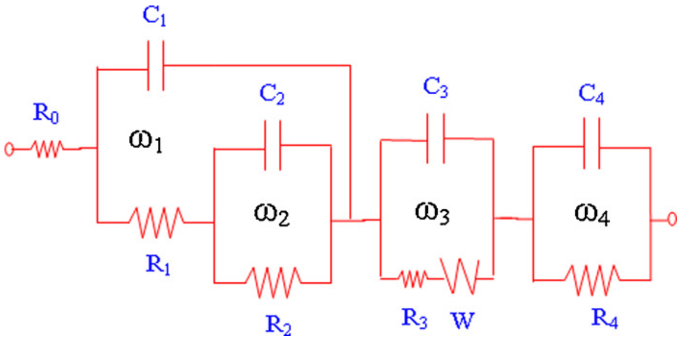

Fig. 7. EC glass structure simulated using an Equivalent circuit where ω_1 and ω_2 represent working electrodes and ω_3 and ω_4 represent the electrolyte and counter electrode.

film can be detected by current density. A larger device had larger impedance. In the colored state of the 25 cm^2 device, which had the greatest impedance, the Li^+ ions were impeded from moving into the WO_3 film within the 30 s charge time (scan from 0 to −3 V). In bleached states, fewer Li^+ ions moved out of the WO_3 film. For example, devices with 1 cm^2, 4 cm^2, 9 cm^2, and 25 cm^2 areas had values of P_1 (1.7 V, 8.34 mA cm^{-2}), P_2 (1.4 V, 5.3 mA cm^{-2}), P_3 (1.3 V, 3.4 mA cm^{-2}), P_4 (1.2 V, 0.27 mA cm^{-2}).

Fig. 7 shows the EC glass structure simulated using an Equivalent circuit, where ω_1 and ω_2 represent the working electrodes and ω_3 and ω_4 represent the electrolyte and counter electrode. In the circuit, the ohmic impedance includes ITO resistance and transport wire resistance (R_0). The working parts of the ITO/WO_3 and WO_3/electrolyte interfaces are presented as $C_1//R_1$ and $C_2//R_2$. The electrolyte presents as $C_3//(R_3 + W)$. The counter part of ITO/electrolyte is presented as $C_4//R_4$. Fig. 8 shows the impedance spectrum in the Nyquist presentation of a WO_3-based EC glass with device sizes of (a) 1 cm^2, (b) 4 cm^2, (c) 9 cm^2, and (d) 25 cm^2, respectively, made by the standard fabrication process. This impedance spectrum consists of ohmic resistance (R_0), which is a starting point on the *X* axis; three arcs (ω_1, ω_2, ω_3), which are in the high frequency range; and one Warburg's diffusion impedance (ω_4), which is an oblique line. Arcs or oblique lines in the Nyquist plot represent the existence of an electrochemical interface. The Nyquist plots show that increasing the device size increases the electrolyte impedance. In Fig. 9, the impedances in the high frequency regions also show that the impedances of working and counter electrodes increased with sample size increases. In the EC glass, the conductive ITO film has lower impedance, but the semi-conductive WO_3 film (logo part) and ionic $LiClO_4$/PC electrolyte present higher impedance. Therefore, most of the

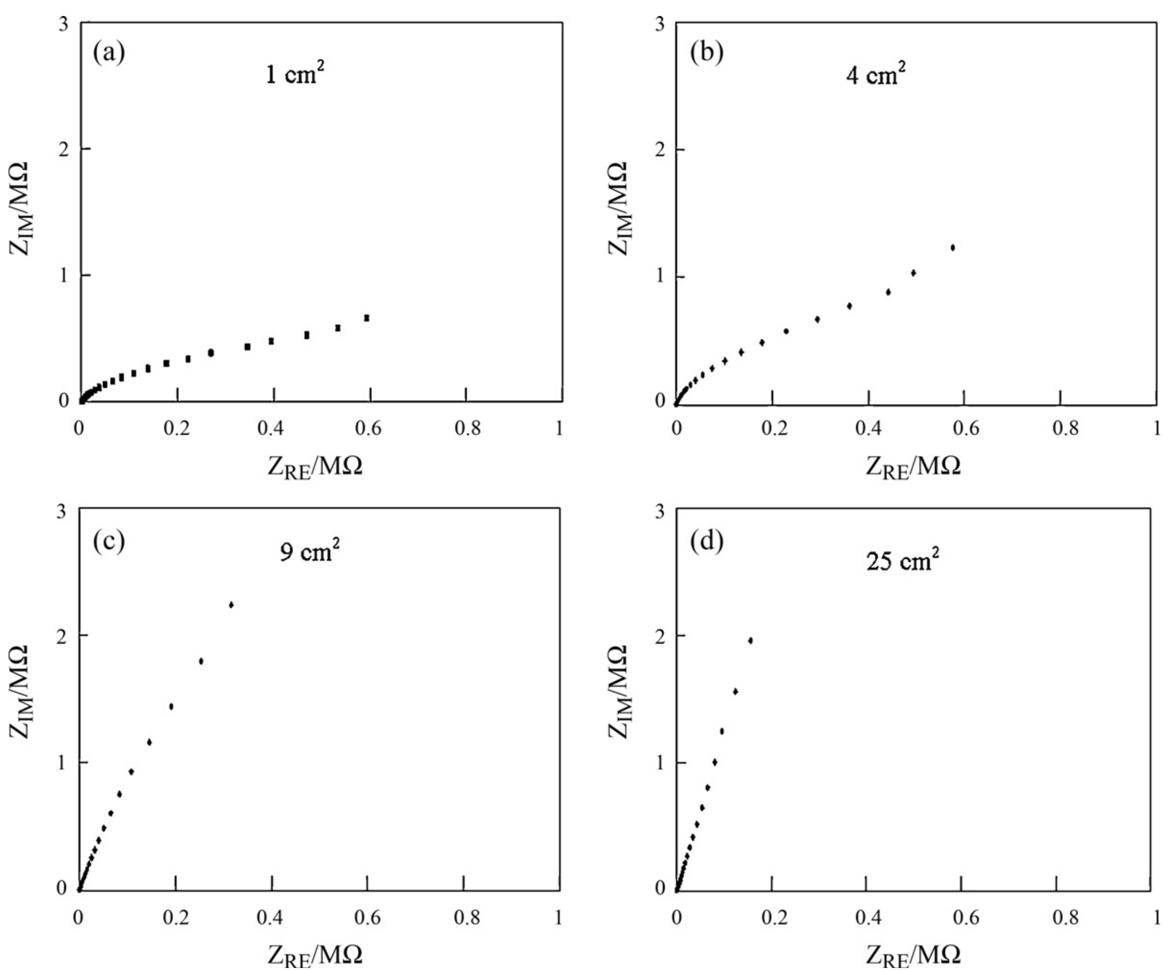

Fig. 8. Nyquist plots of EC glass with device sizes of (a) 1 cm^2, (b) 4 cm^2, (c) 9 cm^2, and (d) 25 cm^2, respectively.

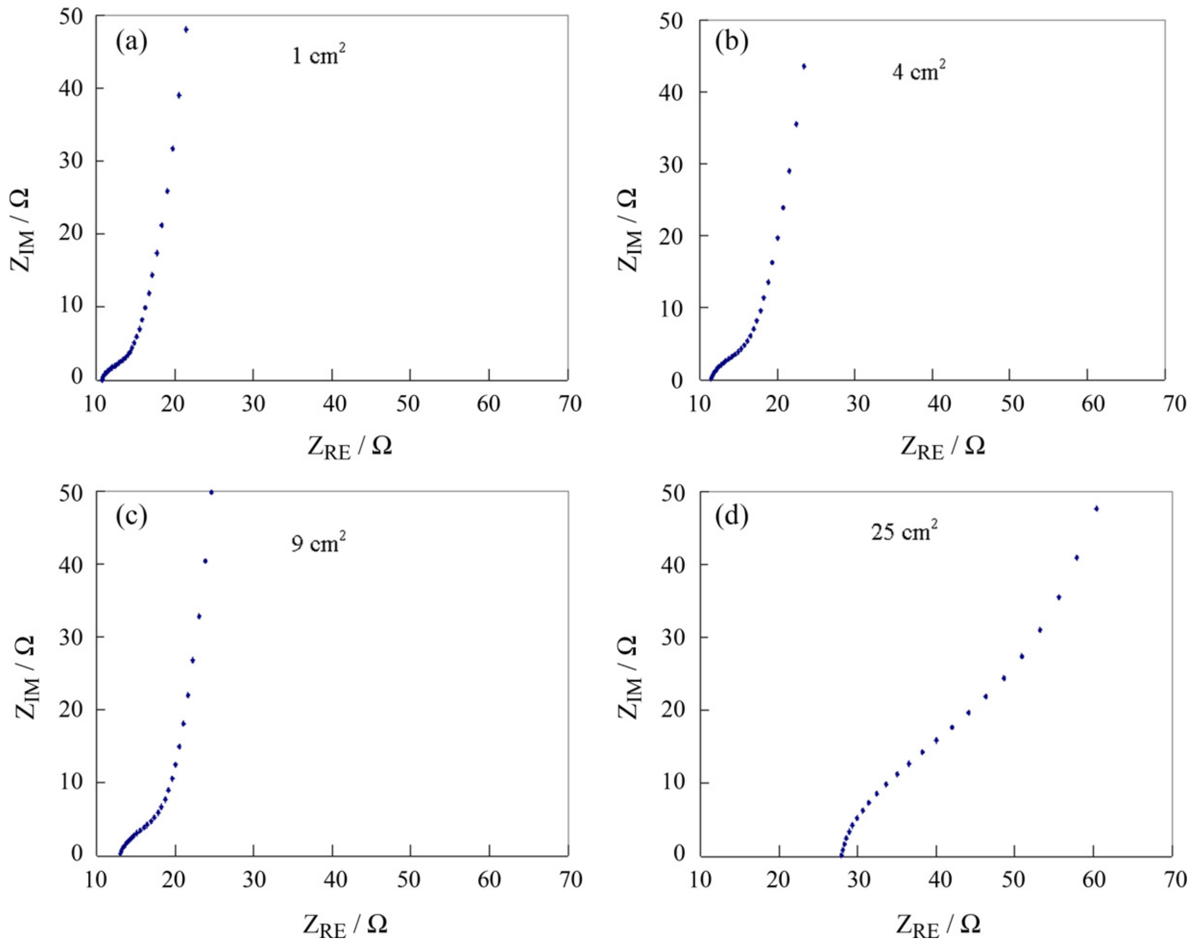

Fig. 9. Nyquist plots of EC glass with device sizes of (a) 1 cm^2, (b) 4 cm^2, (c) 9 cm^2, and (d) 25 cm^2 in high frequencies regions, respectively.

impedance was produced by the logo part of the WO_3 film and electrolyte.

4. Conclusions

Various thicknesses of WO_3 film were deposited on ITO glass to form electrochromic glass. The characteristics of the EC glass were determined using UV–vis transmittance spectra, cyclic voltammetry, and electrochemical impedance spectrum equipment. Alternating logotypes (''NCUT'' and ''NUU'') presented on the electrodes under alternating voltage control when the device was in the negative and positive voltage states. The device with 140 nm WO_3 as the active layer had average transmittances in the colored and bleached states of 11.9% and 54.8%, respectively. The transmittance spectra results showed that a clear color change in the device was observed when the applied voltage was below −3 V (colored) and above 2 V (bleached). The EIS results showed that increasing device size also increased the internal impedances of the working electrode, counter electrode, and electrolyte. Specific logotypes of WO_3 electrochromic films on ITO glass can improve logotype-selective EC glass for application as a functional display controlled by voltage variation.

Acknowledgment

Part of this study was supported by Grants from the National Science Council, Taiwan (99-2627-M-239-001).

References

[1] S. Supothina, P. Seeharaj, S. Yoriya, M. Sriyudthsak, A. Fujishima, Synthesis of tungsten oxide nanoparticles by acid precipitation method, Ceramics International 33 (2007) 931–936.
[2] W. Du, Q. Su, Photochromic fabric of WO_3 and its anti-UV properties, Advanced Materials Research 156–157 (2011) 1301–1304.
[3] X. Zhao, T.L.Y. Cheung, X. Zhang, D.H.L. Ng, J. Yu, Facile preparation of strontium tungstate and tungsten trioxide hollow spheres, Journal of the American Ceramic Society 89 (2006) 2960–2963.
[4] J.L. Solis, S. Saukko, L. Kish, C.G. Granqvist, V. Lantto, Semiconductor gas sensors based on nanostructured tungsten oxide, Thin Solid Films 391 (2001) 255–260.
[5] F.B. Li, G.B. Gu, X.J. Li, H.F. Wan, Preparation, characterization and photo-catalytic behavior of WO_3/TiO_2 nanopowder, Acta Physico-Chimica Sinica 16 (2000) 997–1002.
[6] C. Trimble, M. Devries, J.S. Hale, D.W. Thompson, T.E. Tiwald, J.A. Woollam, Polymer conductor, and nickel oxide, Thin Solid Films 26 (1999) 355–356.
[7] S. Reich, G. Leitus, Y. Tssaba, Y. Levi, A. Sharoni, O. Millo, Localized high-Tc superconductivity on the surface of Na-doped WO_3, Journal of Superconductivity 13 (2000) 855–861.

[8] A. Bailini, F. Di Fonzo, M. Fusi, C.S. Casari, A. Li Bassi, V. Russo, A. Baserga, C.E. Bottani, Pulsed laser deposition of tungsten and tungsten oxide thin films with tailored structure at the nano- and mesoscale, Applied Surface Science 253 (2007) 8130–8135.
[9] Y.G. Choia, G. Sakaib, K. Shimanoeb, Y. Teraokab, N. Miurac, N. Yamazoe, Preparation of size and habit-controlled nano crystallites of tungsten oxide, Sensors and Actuators B: Chemical 93 (2003) 486–494.
[10] U.O. Krasovec, B. Orel, A. Georg, V. Wittwer, The gasochromic properties of sol–gel WO_3 films with sputtered Pt catalyst, Solar Energy 68 (2000) 541–545.
[11] A. Monteiro, M.F. Costa, B. Almeida, V. Teixeira, J. Gago, E. Roman, Structural WO_3 deposited on glass and ITO, Vacuum 64 (2002) 287–291.
[12] E. Ozkan, S.H. Lee, C.E. Tracy, J.R. Pitts, S.K. Deb, Comparison of electrochromic amorphous and crystalline tungsten oxide films, Solar Energy Materials and Solar Cells 79 (2003) 439–448.
[13] S.M. Durrani, E.E. Khawaja, M.A. Salim, M.F. Al-Kuhaili, A.M. Al-Shukri, Effect of preparation conditions on the optical and thermochromic properties of thin films of tungsten oxide, Solar Energy Materials and Solar Cells 71 (2002) 313–325.
[14] Z. Dimitrova, D. Gogova, On the structure, stress and optical properties of CVD tungsten oxide films, Materials Research Bulletin 40 (2005) 333–340.
[15] S. Shingubara, Y. Murakami, H. Sakaue, T. Takahagi, Formation of aluminum nanodot array by combination of nanoindentation and anodic oxidation of aluminum, Surface Science 532–535 (2003) 317–323.
[16] M. Mehmood, A. Rauf, M.A. Rasheed, S. Saeed, J.I. Akhter, J. Ahmad, M. Aslam, Preparation of transparent anodic alumina with ordered nanochannels by through-thickness anodic oxidation of aluminium sheet, Materials Chemistry and Physics 104 (2007) 306–311.
[17] H. Masuda, F. Hasegwa, S. Ono, Self-ordering of cell arrangement of anodic porous alumina formed in sulfuric acid solution, Journal of the Electrochemical Society 144 (1997) L127–L130.
[18] D. Gong, C.A. Grimes, O.K. Varghese, W. Hu, R.S. Singh, Z. Chen, E.C. Dickey, Growth of nano-scale hydroxyapatite using chemically treated titanium oxide nanotubes, Journal of Materials Research 16 (2001) 3331–3334.
[19] H.C. Shin, J. Dong, M. Liu, Porous Tin oxides prepared using an anodic oxidation process, Advanced Materials 16 (2004) 237–240.
[20] I. Sieber, H. Hildebrand, A. Friedrich, P. Schmuki, Formation of self-organized niobium porous oxide on niobium, Electrochemistry Communications 7 (2005) 97–100.
[21] H. Tsuchiya, J.M. Macak, I. Sieber, L. Taveira, A. Ghicov, K. Sirotna, P. Schmuki, Self-organized porous WO_3 formed in NaF electrolytes, Electrochemistry Communications 7 (2005) 295–298.
[22] C.G. Granqvist, Electrochromic tungsten oxide films: review of progress 1993–1998, Solar Energy Materials and Solar Cells 60 (2000) 201–262.
[23] S.M. Montemayor, A.F. Fuentes, Electrochemical characteristics of lithium insertion in several 3D metal tungstates (MWO4, M = Mn, Co, Ni and Cu) prepared by aqueous reactions, Ceramics International 30 (2004) 393–400.
[24] C.M. Lampert, Heat mirror coatings for energy conserving windows, Solar Energy Materials and Solar Cells 6 (1981) 1–41.
[25] R.E. Collins, T.M. Simko, Current status of the science and technology of vacuum glazing, Solar Energy 62 (1998) 189–213.